IOP Publishing Journal of Physics: Condensed Matter
J. Phys.: Condens. Matter **28** (2016) 166003 (8pp) doi:10.1088/0953-8984/28/16/166003

# Europium and manganese magnetic ordering in $EuMn_2Ge_2$

**D H Ryan[1], Rasa Rejali[1], J M Cadogan[2], R Flacau[3] and C D Boyer[3]**

[1] Physics Department and Centre for the Physics of Materials, McGill University, 3600 University Street, Montreal, Quebec, H3A 2T8, Canada
[2] School of Physical, Environmental and Mathematical Sciences, UNSW Canberra at the Australian Defence Force Academy, Canberra, ACT, BC 2610, Australia
[3] Canadian Neutron Beam Centre, Chalk River Laboratories, Ontario, Canada

E-mail: dhryan@physics.mcgill.ca

Received 23 February 2016, revised 3 March 2016
Accepted for publication 4 March 2016
Published 24 March 2016

**Abstract**

The antiferromagnetic structures of both the manganese and europium sublattices in $EuMn_2Ge_2$ have been determined using thermal neutron diffraction. $T_N(Mn) = 714(5)$ K with the 3.35(5) $\mu_B$ (at 285 K) Mn moments ordering according to the $I4'/m'm'm$ space group. The Eu order is incommensurate with the 6.1(2) $\mu_B$ (at 3.6 K) Eu moments oriented parallel to the $c$-axis with a propagation vector of $\mathbf{k} = [0.153(2)\ 0\ 0]$. Both neutron diffraction and $^{151}$Eu Mössbauer spectroscopy reveal evidence of magnetic short-range ordering of the Eu sublattice around and above $T_N(Eu) \sim 10$ K. The ordering temperature of the Eu sublattice is strongly affected by the sample's thermal history and rapid quenching from the melting point may lead to a complete suppression of that ordering.

Keywords: Mössbauer spectroscopy, neutron diffraction, magnetic structure, europium intermetallic compounds

(Some figures may appear in colour only in the online journal)

## 1. Introduction

The tetragonal $ThCr_2Si_2$-type (space group #139 I4/mmm) family of europium compounds ($EuT_2X_2$, where $T$ is a transition metal and X is taken from the silicon group) exhibits a rich variety of behaviour that in many cases can be traced back to the $Eu^{2+} \Leftrightarrow Eu^{3+}$ valence instability. One of the earliest examples of this behaviour was observed in $EuCu_2Si_2$ where a strongly temperature dependent intermediate valence state was reported, with the $Eu^{2+}$:$Eu^{3+}$ balance shifting towards $Eu^{2+}$ with increasing temperature [1]. Remarkably, the details of the valence balance and temperature dependence are strongly sample dependent, and in the most extreme case of indium-flux grown single crystals, the Eu is fully divalent and orders magnetically below 12 K [2].

A simpler and perhaps more reproducible way to study the $Eu^{2+} \Leftrightarrow Eu^{3+}$ valence instability is provided by the pseudo-ternary system: $EuMn_2Si_{2-x}Ge_x$. In $EuMn_2Ge_2$, (i.e. $x = 2$) the Eu is firmly divalent and orders at 13 K [3], but the replacement of the germanium by silicon (i.e. $x \to 0$) drives a $Eu^{2+} \Rightarrow Eu^{3+}$ conversion. By $x = 0.2$ the $Eu^{2+}$:$Eu^{3+}$ balance is approximately 1:1. $EuMn_2Si_2$ exhibits the same temperature dependent valence shift noted above for $EuCu_2Si_2$ [3]. The ordering of the Mn sublattice appears to be largely unaffected by either the Eu valence or the magnetic ordering of the Eu sublattice, with $T_N(Mn)$ decreasing from 395 K at $x = 0$ to 302 K at $x = 2$.

More recently, Hofmann *et al* [4] used neutron diffraction to make direct measurements of the magnetic ordering in $EuMn_2Si_{2-x}Ge_x$ at $x = 0, 2$ and found several surprises. They showed that the magnetic structures adopted by the Mn sublattices in the two compounds were different. Both were simple commensurate antiferromagnetic (AF) structures, but in $EuMn_2Ge_2$ the Mn moments are arranged AF both within the ab-plane and along the $c$-axis (magnetic space group $I4'/m'm'm$), while for $EuMn_2Si_2$ the Mn moments form ferromagnetic ab-sheets that are coupled AF along the $c$-axis (magnetic space group $I_p4/m'm'm'$). As Hofmann *et al* [4]

 

made direct measurements of the Mn magnetic ordering, rather than inferring it from Mössbauer measurements on $^{57}$Fe-doped samples as Nowik *et al* had done [3], they obtained more reliable values for the ordering temperatures for the Mn sublattices. For $EuMn_2Si_2$ ($x = 0$) they found $T_N(Mn) = 391(5)$ K, fully consistent with the previously reported value of 395 K [3]. By contrast, for $EuMn_2Ge_2$ ($x = 2$) they reported $T_N(Mn) = 667(9)$ K (extrapolated from 623 K where their data ended) more than double the 302 K reported previously [3]. However, their most striking result was the absence of any evidence for ordering of the Eu sublattice above 1.8 K. $^{151}$Eu Mössbauer spectroscopy clearly shows that the Eu in $EuMn_2Ge_2$ is ordered with a large (30.9(3) T) hyperfine field at 4.2 K [5]. Ordering temperatures of 9 K [5] and 13 K [3] have been reported, although the basis for these numbers is unclear as in both cases the origin was not stated. Both values are, however, well above the 1.8 K investigated by Hofmann *et al* [4].

Hofmann *et al* [4] used $^{153}$Eu to reduce the impact of the large neutron absorption cross-section associated with the ∼48% $^{151}$Eu present in natural europium. This has several impacts. The first and most obvious is that the sample is necessarily small (∼0.5 g is reported [4]), and this tends to both limit the scattering signal and discourage a more extensive evaluation of the sample (only neutron diffraction results have been reported on their sample [4]). The second is that the sample might not be fully representative of more conventionally prepared samples. Normally this would not be an issue, but in light of the preparation sensitivity noted above, there is a real possibility that even a slight departure from the conditions used in the earlier reports could lead to changes in the magnetic properties, especially for the Eu sublattice. A third impact is that by eliminating $^{151}$Eu from the sample, they precluded the possibility of using $^{151}$Eu Mössbauer spectroscopy to investigate the valence and magnetic behaviour of the Eu sublattice, and to provide direct comparisons with earlier work on this material [3, 5]. While $^{153}$Eu Mössbauer spectroscopy is possible, and does yield the same valence and magnetic information of its more common cousin ($^{151}$Eu), the 103 keV gamma energy makes it rather challenging, and one would normally work with a larger sample than Hofmann *et al* had available [6].

In light of the more than 300 K difference in ordering temperatures reported for the Mn sublattice and the surprising absence of ordering on the Eu sublattice, we decided to re-visit $EuMn_2Ge_2$. A single, large (∼3 g) sample was prepared using natural europium. The entire sample was reduced to powder and sub-samples of the original ingot were used for each of the measurements presented here. We employed a large-area flat-plate technique to reduce the impact of the neutron absorption by the natural europium [7] and this allowed us to use about 2.6 g of material for the neutron diffraction work. We show that the Mn sublattice orders AF at $T_N = 714(5)$ K and we observe incommensurate ordering of the Eu sublattice at $T_N = 9.8(1)$ K. In addition, we demonstrate that the thermal history of the material has a profound impact on the magnetic ordering of the Eu sublattice.

## 2. Experimental methods

The polycrystalline sample of $EuMn_2Ge_2$ was synthesised by argon-arc melting the pure elements (Eu 99.9%, Mn 99.99%, Ge 99.999%) on a water-cooled copper hearth. A 5% excess of Eu was used to compensate for evaporation losses during melting. The sample was then wrapped in tantalum foil, sealed in a quartz tube with a partial pressure of helium, and annealed for 7 days at 900 °C. Sample quality was checked using Cu-$K_\alpha$ x-ray powder diffraction.

The thermal signature of the Mn ordering was measured using a Perkin-Elmer differential scanning calorimeter (DSC–7) with a nickel metal standard providing a transition reference point. AC-susceptibility measurements were made using a quantum design physical properties measurement system (PPMS) at a frequency of 1 kHz and a drive field of 1 mT.

The $^{151}$Eu Mössbauer spectroscopy measurements were carried out using a 4 GBq $^{151}SmF_3$ source, driven in constant acceleration mode. The drive motion was calibrated using a standard $^{57}$CoRh/$\alpha$-Fe foil. The 21.6 keV gamma rays were recorded using a thin NaI scintillation detector. The sample was cooled in a vibration-isolated closed-cycle helium refrigerator with the sample in a helium exchange gas. Temperature stability, as read by a calibrated cernox thermometer, was better than 0.01 K during each measurement. The methods used to fit the $^{151}$Eu Mössbauer spectra are described later, where the data are presented.

Neutron powder diffraction experiments were carried out on the C2 800-wire powder diffractometer (DUALSPEC) at the NRU reactor, Chalk River Laboratories, Ontario, Canada, using neutron wavelengths ($\lambda$) of 1.327 22(17) Å ('short', ∼1.33 Å) and 2.367 62(30) Å ('long', ∼2.37 Å). Diffraction patterns were obtained over the temperature range 3.6–20 K using a closed-cycle helium refrigerator, and from room temperature up to 800 K in a resistively heated furnace with the sample in vacuum.

Natural europium is a strong neutron absorber and its scattering length is dependent on the neutron energy, as tabulated by Lynn and Seeger [8], from which we derived the scattering length coefficient appropriate to our neutron wavelength: $\lambda \sim 1.33$ Å, $E = 46.3$ meV, $b_c = 6.9–0.9i$ fm; and $\lambda \sim 2.37$ Å, $E = 14.6$ meV, $b_c = 7.25–1.52i$ fm.

The sample mounting arrangement for this strongly-absorbing sample employs a large-area, flat-plate geometry as outlined in a previous paper [7] and used by us in neutron diffraction studies of other Eu 1 : 2 : 2 compounds [9, 10]. To facilitate direct comparision with the work of Hofmann *et al* [4] the GSAS/EXPGUI package [11, 12] was used to fit the neutron powder diffraction patterns at and above 20 K where only the AF order of the Mn sublattice was present. As the ordering of the Eu sublattice proved to be incommensurate, and GSAS cannot handle such structures, we used the *FullProf/WinPLOTR* program [13, 14] to fit the Eu ordering. FullProf was also used to fit the x-ray data and to confirm the GSAS analysis of the Mn ordering. The determination of the symmetry-allowed magnetic structures by Representational Analysis used the BASIREPS program [13, 14].

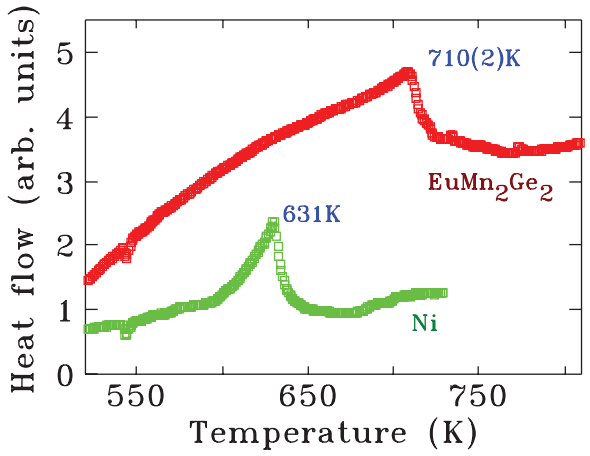


**Figure 1.** Differential scanning calorimetry data for $EuMn_2Ge_2$ (top, red) and a nickel standard (bottom, green), showing the thermal signature of the Mn magnetic ordering at 710(2) K.

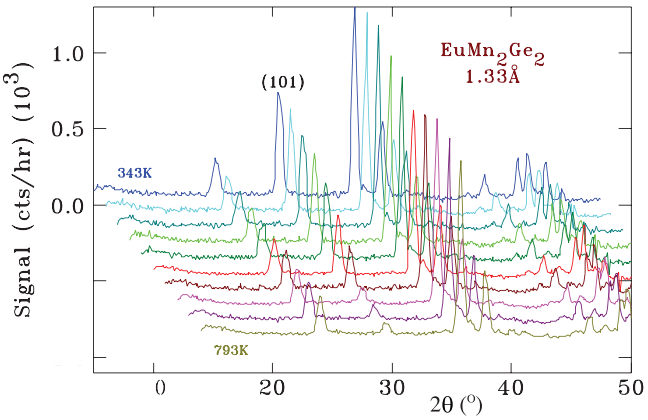


**Figure 2.** Neutron powder diffraction patterns taken at ∼1.33 Å between 343 K and 793 K showing the thermal evolution of the scattered intensity. The most obvious change is in the (1 0 1) peak which is dominated by magnetic scattering from the ordered Mn moments. The patterns have been displaced down and right with increasing temperature, starting with the 343 K pattern in the correct position.

## 3. Results

### *3.1. Initial characterisation*

Analysis of the room temperature x-ray diffraction pattern confirmed that we had obtained the expected tetragonal phase with some small contributions from two impurity phases ($EuGe_2$ (2.9(6) wt.%) and EuO (3.8(6) wt.%)) also being present. Lattice parameters for $EuMn_2Ge_2$ ($a = 4.2450$ (14) Å, $c = 10.882(4)$ Å) were consistent with previous values. Neither impurity affects our analysis of the magnetic ordering of $EuMn_2Ge_2$ as, while both are magnetic, their transition temperatures lie well outside our primary ranges of interest. EuO orders ferromagnetically at 69 K [15] and so yields no new reflections. $EuGe_2$ is AF with $T_N = 48$ K [16]. The moments lie in the ab-plane and the structure is doubled along the *c*-axis [17]. The additional magnetic contributions do not overlap with those of $EuMn_2Ge_2$ and were included in our fits.

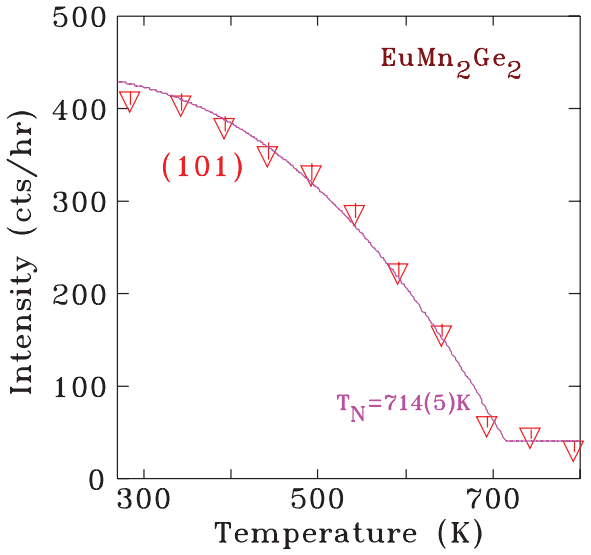


**Figure 3.** Temperature dependence of the (1 0 1) peak intensity. The solid line is a fit to a $J = \frac{5}{2}$ squared Brillouin function giving a transition temperature of 714(5) K, fully consistent with our DSC data. Note: the intensity of the (1 0 1) peak does not go to zero above $T_N$ because there is also a small nuclear contribution at this position.

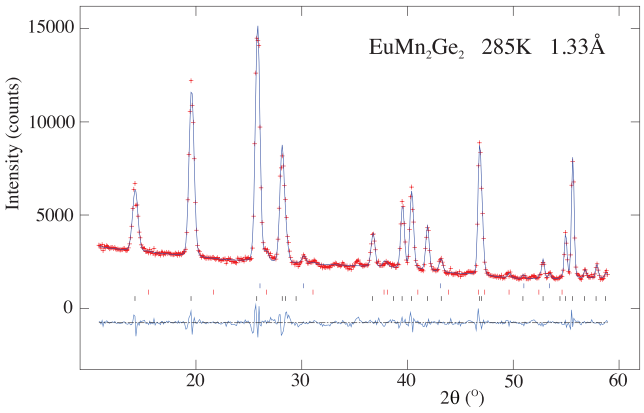


**Figure 4.** 285 K neutron powder diffraction pattern of $EuMn_2Ge_2$ taken at $\lambda = 1.327\,22(17)$ Å. The Bragg markers show (from top to bottom): EuO (blue), $EuGe_2$ (red) and $EuMn_2Ge_2$ (black).

An initial determination of the Mn ordering temperature was made using differential scanning calorimetry with pure nickel providing a reference standard to correct for any calibration errors or phase lags associated with the 40 K $min^{-1}$ heating rate. The thermal signature of the Mn ordering is clearly visible in figure 1 and yields an ordering temperature of 710(2) K, far higher than the 302 K reported by Nowik *et al* [3], and more consistent with, if somewhat higher than, the 667(9) K obtained by extrapolation by Hofmann *et al* [4].

Low-temperature ac susceptibility (1 kHz, 1 mT) revealed a roughly 1/T increasing behaviour with a clear peak centred at 9.2(1) K. The position of the susceptibility peak is reasonably consistent with the 10 K–13 K ordering temperature expected for the Eu sublattice. We defer discussion of possible Eu ordering until after that of the Mn sublattice.

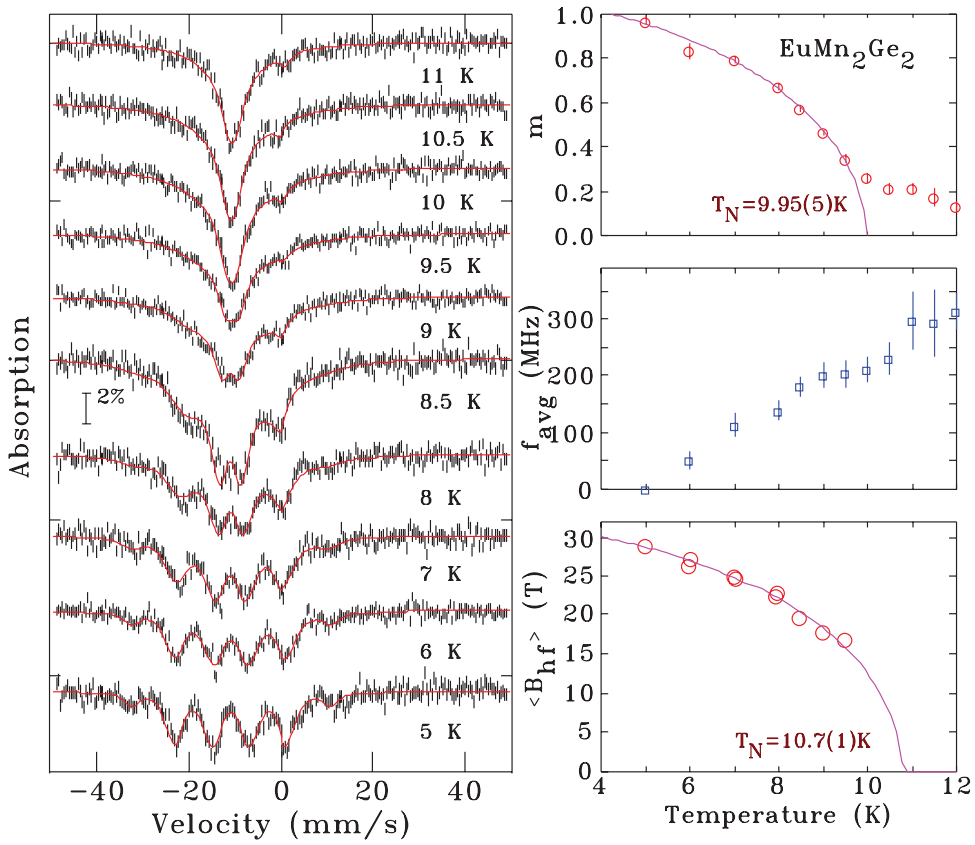


**Figure 5.** Left panel: $^{151}$Eu Mössbauer spectra of $EuMn_2Ge_2$ measured between 11 K and 5 K showing the development of magnetic order. The feature near 0 mm s$^{-1}$ evident above 9 K is due to the presence of $Eu_2O_3$, likely introduced during grinding. The solid lines are dynamic fits described in the text. Right panel: (top) average magnetisation and (centre) fluctuation rate derived from dynamic fits; (bottom) average hyperfine field derived from the modulated distribution fits. The fits used to obtain the two estimates of the transition temperature are described in the text.

### 3.2. Manganese ordering

Sections of the neutron diffraction patterns for $EuMn_2Ge_2$ taken above room temperature at a wavelength of $\lambda = 1.327\,22(17)$ Å are shown in figure 2. The (1 0 1) peak near $2\theta = 30°$ has the largest contribution from the Mn ordering. Tracking the intensity of this peak (figure 3) and fitting its temperature dependence with a conventional $J = \frac{5}{2}$ squared Brillouin function yields an ordering temperature of 714(5) K, fully consistent with that derived from differential scanning calorimetry above.

Analysis of the 285 K neutron diffraction pattern of $EuMn_2Ge_2$ taken at a wavelength of 1.327 22(17) Å was initially carried out using the GSAS/EXPGUI package [11, 12] for consistency with Hofmann *et al* [4]. Refinement using the $I4'/m'm'm$ magnetic space group gave a Mn moment of 3.35(5) $\mu_B$ at 285 K, rising to 3.47(6) $\mu_B$ at 20 K. The refined pattern at 285 K is shown in figure 4. As the Eu order is incommensurate (*vide infra*), we also used the *FullProf/WinPLOTR* program suite [13, 14] to fit the Mn ordering in preparation for including that of the Eu. This analysis gave an equivalent description of the Mn order at 285 K: 3.55(15) $\mu_B$ Mn moments aligned along the *c*-axis in the $\Gamma_7^{(1)}$ representation ordered with a propagation vector of [0 0 0]. Both our magnetic structure and the Mn moments derived from our fits are in full agreement with the work of Hofmann *et al* [4].

### 3.3. Europium ordering

*3.3.1. $^{151}$Eu Mössbauer spectroscopy.* The room temperature $^{151}$Eu Mössbauer spectrum of $EuMn_2Ge_2$ consists of a single sharp line. Fitting yields an isomer shift of −10.84(3) mm s$^{-1}$ confirming that the Eu is fully divalent. On cooling to 5 K the line splits into a clearly magnetic pattern with a hyperfine field ($B_{hf}$) of 30.2(2) T suggesting that the Eu in our sample does indeed order. Both our room temperature isomer shift and 5 K hyperfine field are fully consistent with those reported by Felner and Nowik [5]. Unfortunately, no such measurements were possible for the neutron diffraction sample prepared by Hofmann *et al* [4] as it was made using isotopically separated $^{153}$Eu.

It is apparent from the spectra shown in figure 5. that the thermal evolution of the Eu order is not simple: a fixed-linewidth, single site fit does not reproduce the observed behaviour. The lines broaden and the spectrum collapses towards the centre on warming (most obvious at 8.5 K), and significant broadening persists even to 50 K. Two approaches were used to fit the spectra. Given the previous failure to detect long-ranged

magnetic ordering of the Eu sublattice [4] and the form of the spectra in figure 5, we first considered the possibility that the Eu undergoes slow paramagnetic relaxation rather than developing full static order. A dynamic two-state Blume and Tjon model was therefore used to analyse the spectra [18].

As can be seen in figure 5 (right centre), the relaxation rate derived from the fits increases steadily with increasing temperature. We found that a biassed relaxation model (unequal times spent in the 'up' and 'down' states) provided a better fit to the data and the derived magnetisation could be fitted using a conventional $J = \frac{7}{2}$ Brillouin function up to ∼9.5 K, to yield an ordering temperature of $T_N$(Eu) ∼ 10 K, although there are significant departures from the expected behaviour above 10 K, and the spectra remains visibly broadened above the fitted transition temperature. While this simple dynamic model does reproduce the gross behaviour, it does not yield consistently good fits to the spectra at all temperatures (the misfit at 8.5 K is quite clear).

Another approach that was tried in light of the incommensurate Eu ordering observed by neutron diffraction below, models the spectral shape using a distribution of hyperfine fields derived from an (assumed) incommensurate sinusoidally modulated magnetic structure [19]. By adding higher harmonics it is possible to allow for a gradual squaring up of the modulation. This model has been used to fit $^{151}$Eu Mössbauer spectra of EuPdSb [20], $EuNiGe_3$ [19] and $Eu_4PdMg$ [21]. Applying this model to the spectra shown in figure 5 yields a rapid development of a sinusoidal modulation on heating from 5 K and fitting the average magnitude of the hyperfine field ($\langle|B_{hf}|\rangle$) as a function of temperature gives a transition temperature of $T_N$(Eu) = 10.7(1) K; however, the model fails to account for the observed spectral shape by 9 K where dynamic behaviour appears to dominate.

Both Mössbauer-based estimates of the Eu ordering temperature are broadly consistent with the $T_N$(Eu) = 9.2(1) K derived from ac susceptibility data. Given the complex behaviour implied by the temperature evolution of the $^{151}$Eu Mössbauer spectra, it is not surprising that the agreement on $T_N$(Eu) is not perfect.

Contrary to the earlier findings of Hofmann *et al* [4], our $^{151}$Eu Mössbauer data clearly suggest that the Eu moments order below about 10 K in $EuMn_2Ge_2$. They also point to a complex mix of an incommensurate modulation of that order, with slow paramagnetic dynamics that persist well above the estimated ordering temperature. For a modulation to be meaningful, the moments would have to be correlated over a significant distance, however the observation of dynamics could indicate that the order may not be truly static. We therefore turn to neutron diffraction to determine the actual nature of the static, long-ranged order, if it exists.

*3.3.2. Neutron diffraction.* Comparison of neutron powder diffraction patterns taken at 20 K and 3.6 K using a wavelength of ∼2.37 Å presented in figure 6 clearly shows that the Eu moments in $EuMn_2Ge_2$ do indeed order. While there are a significant number of new, magnetic peaks evident in the difference pattern at the bottom of figure 6, the 3.6 K

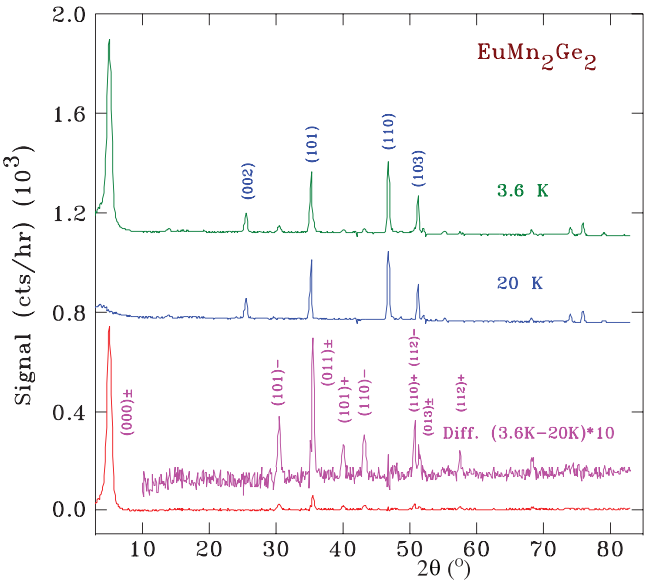


**Figure 6.** Neutron powder diffraction patterns for $EuMn_2Ge_2$ measured with a wavelength of ∼2.37 Å and taken at 3.6 K (top) and 20 K (middle) showing the development of magnetic scattering from the ordered Eu moments (most notably at $2\theta = 5°$). The bottom pattern shows the difference between the 20 K and 3.6 K data with a section multiplied by a factor of ten to make the many weaker magnetic peaks more apparent. Several of the strongest nuclear (in blue) and magnetic (in magenta) reflections are indexed.

diffraction pattern is dominated by a large (about three times the intensity of any other peak in the pattern) peak at $2\theta \sim 5°$ that corresponds to a d-spacing of about 27.4 Å. This peak is incommensurate, and as we show below, can be indexed as the $(0\,0\,0)^{\pm}$ peak with a propagation vector of $\mathbf{k} = [0.153(2)\ 0\ 0]$. That the primary magnetic peak occurs at so low an angle when working with ∼2.37 Å neutrons, serves to emphasise the advantages of our flat plate technique [7] in permitting us to work with quite long wavelength neutrons, moving peaks from long-period structures out to accessible scattering angles.

A fit to the temperature dependence of the $(0\,0\,0)^{\pm}$ peak intensity shown in the lowest panel of figure 7 gives an ordering temperature of 9.8(1) K, fully consistent with the estimates derived above from fits to our $^{151}$Eu Mössbauer data. We found that a $J = \frac{1}{2}$ squared Brillouin function gave a much better fit than the $J = \frac{7}{2}$ form that might be expected for $Eu^{2+}$, and this likely reflects some axial anisotropy associated with the *c*-axis ordering. Figure 7 also shows that the position of the $(0\,0\,0)^{\pm}$ peak changes on warming towards $T_N$(Eu) and that it broadens significantly. The latter change suggests that the event at $T_N$(Eu) is not a conventional second-order magnetic phase transition, and that shorter-ranged magnetic correlations develop on approaching $T_N$(Eu) from below. This would also be consistent with the complex behaviour observed in the $^{151}$Eu Mössbauer spectra shown in figure 5. Taken together, the Mössbauer and neutron diffraction data suggest that short-ranged magnetic order develops slightly below $T_N$(Eu) and persists well above $T_N$(Eu) (at least as far as 50 K, where we still observe some line broadening).

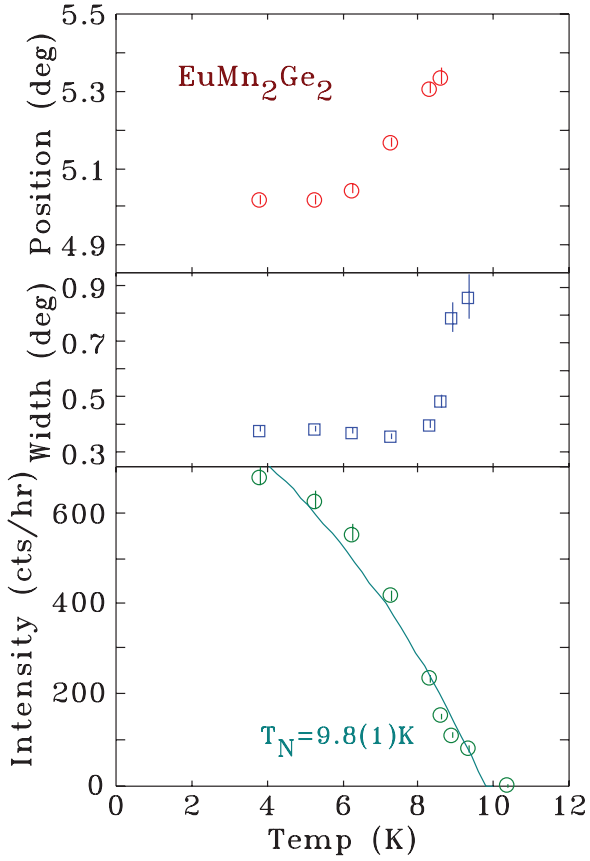


**Figure 7.** Temperature dependence of (top) position (middle) width and (bottom) intensity of the $(0\ 0\ 0)^{\pm}$ magnetic peak from the Eu ordering. Note the significant changes in width and position as $T_N$ is approached from below. The solid line through the intensity data is a fit to a $J = \frac{1}{2}$ squared Brillouin function giving $T_N = 9.8(1)$ K.

**Table 1.** Representational analysis for the Eu(2a) site in $EuMn_2Ge_2$ with a propagation vector [0.153(2) 0 0].

| Representation | Ordering |
|---|---|
| $\Gamma_2^{(1)}$ | $[x\ 0\ 0]$ |
| $\Gamma_3^{(1)}$ | $[0\ 0\ z]$ |
| $\Gamma_4^{(1)}$ | $[0\ y\ 0]$ |

*Note*: The atomic position of the basis Eu moment is (0 0 0).

Representational analysis using the BASIREPS program gives the magnetic representation for the Eu(2a) site, comprising three 1-dimensional representations:

$$\Gamma_{\text{Mag}}^{2a} = 1\Gamma_2^{(1)} + 1\Gamma_3^{(1)} + 1\Gamma_4^{(1)} \quad (1)$$

and the basis vectors of these irreducible representations are given in table 1.

The best refinement to the 3.6 K diffraction pattern has the Eu(2a) sublattice ordered with a propagation vector [0.153(2) 0 0] and the moments aligned along the *c*-axis in the $\Gamma_3^{(1)}$ representation. The refined Eu magnetic moment amplitude at 3.6 K is 6.1(2) $\mu_B$. The refined lattice parameters at 3.6 K are $a = 4.240(2)$ Å and $c = 10.847(6)$ Å. The conventional *R*-factors for this refinement are $R(\text{Bragg}) = 15.0$, $R(F) = 8.5$ and $R(\text{mag}) = 6.3$. The fitted diffraction patterns taken at 3.6 K using wavelengths of ∼2.37 Å and ∼1.33 Å are shown in figure 8.

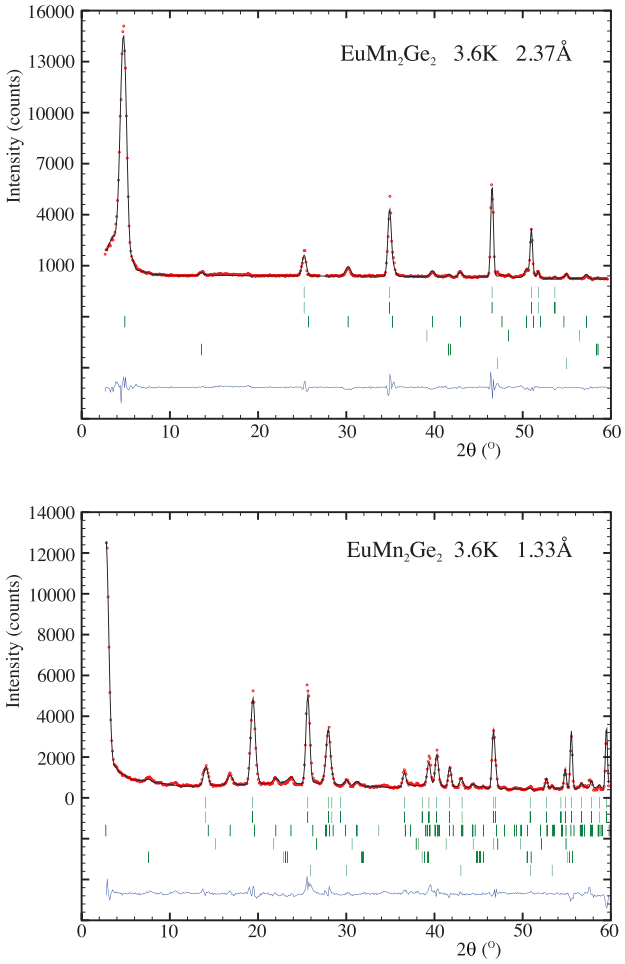


**Figure 8.** 3.6 K neutron powder diffraction pattern of $EuMn_2Ge_2$ taken at (top) $\lambda \sim 2.37$ Å and (bottom) $\lambda \sim 1.33$ Å. In both cases the Bragg markers are (top to bottom): $EuMn_2Ge_2$ (nuclear); $EuMn_2Ge_2$ (Mn magnetic); $EuMn_2Ge_2$ (Eu magnetic); $EuGe_2$ (nuclear); $EuGe_2$ (Eu magnetic); EuO.

We found no evidence for satellite peaks that would reflect the presence of harmonics above the fundamental, suggesting that the magnetic structure is sinusoidally modulated rather than square-wave. The thermal evolution of the $^{151}$Eu Mössbauer spectra in figure 5 certainly supports the presence of a dominant sinusoidal mode to the order, at least as far as 9 K, above which temperature dynamic behaviour rapidly takes over. A number of other models including square-wave and conical structures were tried, but all gave visibly poorer fits. Finally, we note in passing that the magnetic representations of the Mn and Eu orderings are quite different. While it would be better to use a common symmetry to describe the crystal and two magnetic structures, the factor of 70 difference between the two ordering temperatures for the Mn and Eu sublattices indicates that their ordering is far from cooperative, and so a common description should not be expected.

## 4. Discussion

It is clear that the ordering of the Mn sublattice in $EuMn_2Ge_2$ occurs well above the 302 K reported by Nowik *et al* [3] as the thermal and neutron diffraction signatures yield values of

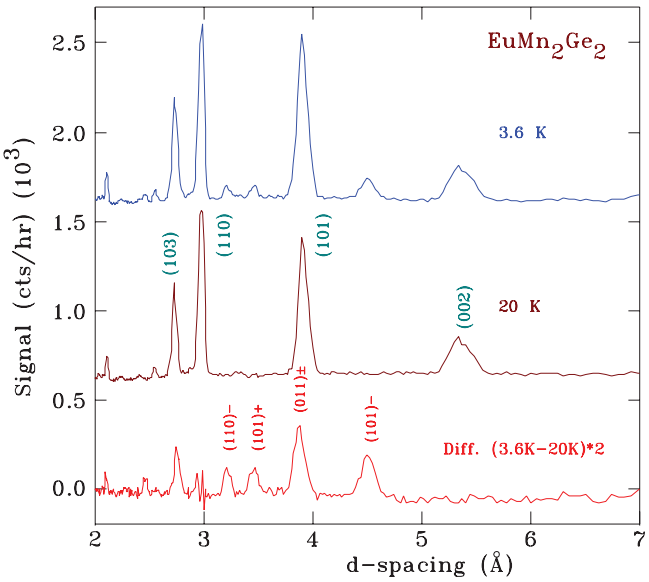


**Figure 9.** Neutron powder diffraction patterns for $EuMn_2Ge_2$ taken at a wavelength of ∼1.33 Å and plotted as d-spacing rather than scattering angle to facilitate comparison with figure 1 of Hofmann *et al* [4]. The figures show the results: (top) at 3.6 K, below the ordering temperature of the Eu moments, (middle) at 20 K, where only the Mn moments are ordered, (bottom) the difference between the 3.6 K and 20 K patterns emphasising the magnetic scattering from the ordered Eu moments. The indices of several key nuclear (on the 20 K pattern) and magnetic (on the difference pattern) reflections are given.

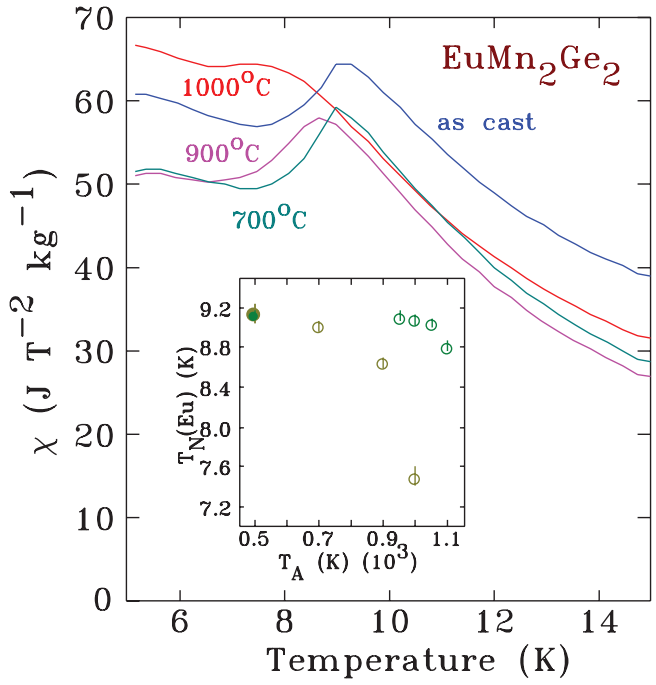


**Figure 10.** AC-susceptibility data for four samples of $EuMn_2Ge_2$ derived from the same initial ingot but annealed and quenched from different temperatures. The inset shows the rapid decrease in the transition temperature ($T_N$(Eu)) with increasing annealing temperature for two series of samples: pressed powders (olive) and ingot pieces (green) (in each case the 'as cast' sample is plotted as a solid point at 500 K for convenience, but no significance should be attached to this choice).

710(2) K and 714(5) K respectively. Our value is somewhat higher than the 667(9) K reported by Hofmann *et al* [4], however their value is derived from an extrapolation from ∼620 K (well below $T_N$) using a critical scaling form. Attempts to re-fit the data presented in their figure 2 employing the Brillouin functions used to fit our data yield transitions at 713(13) K (intensity) and 740(20) K (moment), consistent with our result. We emphasise that while we are revising the transition temperature up, we fully agree with their previously determined magnetic structure ($I4'/m'm'm$).

The contradiction on the Eu ordering is a bigger problem. Re-plotting our diffraction patterns in terms of d-spacing (figure 9) facilitates comparison with figure 1 of Hofmann *et al* [4]. It is clear that while they would not have seen the $(0\,0\,0)^{\pm}$ peak, several other peaks do occur within the range covered by their measurements (most notably the $(1\,0\,1)^{-}$ at $d \sim 4.5$ Å) and assuming that the statistical quality of their patterns taken below 10 K were comparable to that shown for 398 K in their figure 1, Hofmann *et al* should have seen the ordering of the Eu sublattice. We are therefore forced to conclude that the Eu in their sample *did not order*, and the question becomes: why not?

It has been shown that growth conditions can profoundly affect the magnetic properties of the Eu in both $EuCu_2Si_2$ [1, 22] and $EuCu_2Ge_2$ [5, 23]. In the silicides, $EuCu_2Si_2$ [1] and $EuMn_2Si_2$ [3], the valence of the Eu is strongly temperature dependent, becoming more divalent with increasing temperature. Substituting germanium for silicon in $EuCu_2Si_{2-x}Ge_x$ also drives the Eu towards a stable divalent state [3]. Finally our analysis of the $^{151}$Eu Mössbauer data shown in figure 5 suggests the presence of slow paramagnetic dynamics and the persistence of some short-ranged correlations above $T_N$(Eu). These observations all point to a potentially fragile Eu state in $EuMn_2Ge_2$ that might be sensitive to variations in the preparation conditions.

To investigate the possibility that the rather small (0.5 g) sample prepared by Hofmann *et al* [4] might have been affected by its thermal history (a small sample might be expected to cool faster in an arc furnace than the larger, multi-gram samples more commonly prepared) we prepared a series of small samples by grinding part of a 2 g arc-melted ingot and pressing the powder in ∼250 mg lots. These were then wrapped in tantalum foil and annealed at 700 °C, 900 °C, and 1000 °C in sealed quartz tubes under a partial pressure of helium. After three days (seven days for the sample annealed at 700 °C) they were water quenched and $^{151}$Eu Mössbauer spectra were taken at ambient temperature to check for a change in Eu valence. None was found. The observed isomer shifts for the four samples differed by at most 0.06 mm s$^{-1}$ with fitted uncertainties of 0.02 mm s$^{-1}$: i.e. they were the same within error. Similarly, analysis of the x-ray diffraction patterns showed no change in structure, lattice parameters or cell volume. However, susceptibility provided remarkably clear evidence for a quenching effect on the magnetic behaviour. As can be seen in figure 10, quenching from progressively higher temperatures leads to a systematic reduction in $T_N$(Eu) (see inset to figure 10) and a clear weakening of the peak marking the transition. A second series of quenched samples was prepared by using ∼200 mg

solid pieces broken from a new arc-melted ingot. They were sealed, annealed (950 °C–1100 °C) and quenched in the same way. The observed transition temperatures (see inset to figure 10) show a clear but weaker decrease with increasing annealing temperature, although the two as-cast samples are identical. As we have very little real control over the actual quench profile of the samples when the tubes are dropped into a water bath, we attribute the differences between the two series to variations in cooling rate.

Thus, it is clear that the thermal history of $EuMn_2Ge_2$ has a profound effect on the ordering behaviour of the Eu sublattice in $EuMn_2Ge_2$. We believe that the small sample prepared by Hofmann *et al* [4] cooled more rapidly in the arc-furnace, and as a result, was effectively prepared at a higher temperature than the much larger samples prepared by us in this work and others also working on this system. The hitherto unsuspected sensitivity of the Eu ordering in $EuMn_2Ge_2$ to the thermal history of the sample led to them preparing a simple in which the Eu did not order.

## 5. Conclusions

The Mn sublattice in $EuMn_2Ge_2$ orders AF at $T_N(Mn) = 714(5)$ K, adopting a $I4'/m'm'm$ magnetic structure, fully consistent with the previous work of Hofmann *et al* [4]. However, while a previous neutron diffraction study of a sample prepared using isotopically separated $^{153}Eu$, to reduce the effects of neutron absorption, reported no ordering of the Eu sublattice above 1.8 K [4], the results obtained here on a much larger sample prepared using natural europium and a large area flat-plate mounting technique [7], clearly show long-ranged magnetic ordering of the Eu sublattice in $EuMn_2Ge_2$ below $T_N(Eu) = 10$ K. The Eu order is incommensurate, with the moments along the *c*-axis and a propagation vector of $\mathbf{k} = [0.153(2)\ 0\ 0]$. Both neutron diffraction and $^{151}Eu$ Mössbauer spectroscopy point to the development of magnetic short ranged order around and above $T_N(Eu)$ suggesting that the ordering behaviour of the Eu moments does not follow a conventional second-order phase transition. Quenching small samples from progressively higher temperatures leads to a marked reduction in the Eu ordering temperature, pointing to a remarkable sensitivity to thermal history in $EuMn_2Ge_2$. The interplay between the complex ordering behaviour and the sensitivity to preparation details lies behind the previous failure to observe the ordering of the Eu sublattice in $EuMn_2Ge_2$ [4].

The frequency with which complex, incommensurate modulated magnetic structures are showing up in Eu compounds [10, 19, 21, 24], and the remarkable sensitivity to preparation conditions that many Eu compounds exhibit [1, 5, 22, 23] suggests that while $Eu^{2+}$ has the same basic electronic configuration as $Gd^{3+}$ its range of magnetic behaviour in intermetallic compounds is much wider, leading to a richer and more interesting phenomenology. It is unfortunate that magnetic ordering in europium-based compounds has been neglected due to a perceived neutron absorption problem.

## Acknowledgments

Financial support for this work was provided by the Natural Sciences and Engineering Research Council of Canada, the Fonds Québécois de la Recherche sur la Nature et les Technologies and The University of New South Wales. DHR acknowledges the award of a Rector-funded Visiting Fellowship by UNSW Canberra.

## References

[1] Bauminger E R, Froindlich D, Nowik I, Ofer S, Felner I and Mayer I 1973 *Phys. Rev. Lett.* **30** 1053
[2] Wang P, Stadnik Z M, Żukrowski J, Cho B K and Kim J Y 2010 *Phys. Rev.* B **82** 134404
[3] Nowik I, Felner I and Bauminger E R 1997 *Phys. Rev.* B **55** 3033
[4] Hofmann M, Campbell S J and Edge A V J 2004 *Phys. Rev.* B **69** 174432
[5] Felner I and Nowik I 1978 *J. Phys. Chem. Solids* **39** 767
[6] van Lierop J, Voyer C J, Shendruk T N, Ryan D H, Cadogan J M and Cranswick L 2006 *Phys. Rev.* B **73** 174407
[7] Ryan D H and Cranswick L M D 2008 *J. Appl. Cryst.* **41** 198
[8] Lynn J E and Seeger P A 1990 *At. Data Nucl. Data Tables* **44** 191
[9] Ryan D H, Cadogan J M, Xu S, Xu Z and Cao G 2011 *Phys. Rev.* B **83** 132403
[10] Rowan-Weetaluktuk W N, Lemoine P, Cadogan J M and Ryan D H 2014 *J. Appl. Phys.* **115** 17E101
[11] Larson A C and Von Dreele R B 2000 *Report LAUR* 86–748 Los Alamos National Laboratory
[12] Toby B H 2001 *J. Appl. Cryst.* **34** 210–3
[13] Rodríguez-Carvajal J 1993 *Physica* B **192** 55–69
[14] Roisnel T and Rodríguez-Carvajal J 2001 *Mater. Sci. Forum* **378–81** 118–23
[15] Passell L, Dietrich O W and Als-Nielsen J 1976 *Phys. Rev.* B **14** 4897
[16] Bobev S, Bauer E D, Thompson J D, Sarrao J L, Miller G J, Eck B and Dronskowski R 2004 *J. Solid State Chem.* **177** 3545
[17] Cadogan J M, Ryan D H, Rejali R and Boyer C B 2016 *J. Alloys Compd.* submitted
[18] Blume M and Tjon J A 1965 *Phys Rev.* **165** 446
[19] Maurya A, Bonville P, Thamizhavel A and Dhar S K 2014 *J. Phys.: Condens. Matter* **26** 216001
[20] Bonville P, Hodges J A, Shirakawa M, Kasaya M and Schmitt D 2001 *Eur. Phys. J.* B **21** 349
[21] Ryan D H, Legros A, Niehaus O, Pöttgen R, Cadogan J M and Flacau R 2015 *J. Appl. Phys.* **117** 17D108
[22] Stadnik Z M, Wang P, Żukrowski J and Cho B K 2006 *Hyperfine Interact.* **169** 1295
[23] Wang P, Stadnik Z M, Żukrowski J, Cho B K and Kim J Y 2010 *Solid State Commun.* **150** 2168
[24] Lemoine P, Cadogan J M, Ryan D H and Giovannini M 2012 *J. Phys.: Condens. Matter* **24** 236004